Syntheses, Structures, Photoluminescence and Theoretical Studies of Xanthone in Crystalline Resorcinarene-Based Inclusion Complexes

Shao-Liang Zheng* and Philip Coppens*[a]

Abstract: Two new crystalline resorcinarene-based xanthone inclusion complexes, CECR·xanthone·MeOH (**1**), and HECR·2 xanthone·6 MeOH (**2**) (CECR = *C*-ethylcalix[4]resorcinarene, HECR = hexaethylresorcin[6]arene) have been prepared to study the relation between photophysical properties and solid-state structure. Compared with the neat crystals, the xanthone phosphorescence is severely quenched in both solids, but the lifetime is an order of magnitude larger in **2**, in which xanthone occurs as a dimer, than in **1**, in which it occurs as a monomer. The electronic transitions involved in the photoluminescent process, and the relation between the energy levels of host and guest and emission quenching of the guest in the supramolecular solid have been investigated by means of time-dependent density functional theory (TDDFT) calculations.

Keywords: density functional calculations · energy transfer · host–guest systems · inclusion compounds · luminescence

Introduction

Unlike in solutions or rigid glasses, which traditionally have been used for dilution of photoactive species, three-dimensional periodicity is preserved in multicomponent supramolecular solids. Supramolecular host matrixes provide a well-defined environment in which the encapsulated luminescent guest molecules may occur in different states of aggregation and orientation relative to their environment, offering the opportunity to study the structure dependence of photophysical properties.

When supramolecular host–guest inclusion complexes are formed in aqueous solutions an enhancement of the luminescence is often observed.[1] This is partly a result of the elimination of quenching of molecular triplet states by dissolved O_2 molecules, but is also attributed to the change from the polar environment of aqueous solution to the apolar walls of the cavity, as for instance in cyclodextrin inclusion complexes. The first reported example concerns the tenfold increase in fluorescence yield of 1-aninilino-8-naphthalene sulfonate upon inclusion in β- or γ-cyclodextrin.[2] While there are many other examples of luminescence enhancement, with variation of the solvent both an increase and a decrease of the fluorescence intensity of pyrene[3] and xanthone[4] on complexation with α-, β-, and γ-cyclodextrin has been reported. A difficulty in the interpretation of such studies is that the geometry of complexation is not known. There is in fact evidence that an equilibrated array of discrete conformations rather than a single conformation exists in solution.[5] In supramolecular solids on the other hand, the geometry can be determined and collision-induced quenching is eliminated.

Solid-state spectroscopic[6–8] and time-resolved diffraction results[9] show that the excited-state geometry and lifetime are affected by the constraining environment of multicomponent supramolecular solids. Luminescence quenching occurs in the solid state through nonradiative energy or electron transfer between the excited entity and its environment. Control of luminescence quenching and the corresponding enhancement of the light-emission has technological applications in the design of light-emitting diodes,[7,8] and is required for time-resolved diffraction studies of transient species in supramolecular environments.[10] However, few systematic investigations on the relation between structure and properties have been carried out as extensive structural information is only now becoming available[11] and computational techniques have only recently allowed reliable calculations of larger molecules.

[a] Dr. S.-L. Zheng, Prof. Dr. P. Coppens
Department of Chemistry
State University of New York at Buffalo
Buffalo, New York, 14260–3000 (USA)
Fax: (+1) 716-645-6948
E-mail: coppens@buffalo.edu

Supporting information for this article is available on the WWW under http://www.chemeurj.org/ or from the author.

 DOI: 10.1002/chem.200500033 © 2005 Wiley-VCH Verlag GmbH & Co. KGaA, Weinheim

Aromatic ketones, such as benzil,[12–14] benzophenone,[15,16] and xanthone,[17,18] are of particular interest owing to their roles in photophysics and photochemistry. They have excited triplet states with lifetimes that can be as high as milliseconds at low temperature in the solid state,[12,15] and are highly reactive. However, in a series of supramolecular solids based on resorcinarene and bipyridyl-type linker molecules, the intense phosphorescence of the aromatic ketones was found to be completely[13,16] or very strongly[14] quenched, even at low temperature.

As part of our investigations of emission quenching in supramolecular environments we have synthesized two resorcinarene-based inclusion complexes in which no molecules other than the guest and the resorcinarene are present, thus simplifying the analysis. We here describe the syntheses, structures, and photophysical properties of CECR·xanthone·MeOH (**1**), and HECR·2 xanthone·6 MeOH (**2**) (CECR = *C*-ethylcalix[4]resorcinarene, HECR = hexaethylresorcin[6]arene, Scheme 1). The xanthone molecule occurs as monomer in **1** and as a dimer in **2**, resulting in significant variation of the spectral properties. The experimental work is complemented by calculations based on time-dependent density functional theory (TDDFT).

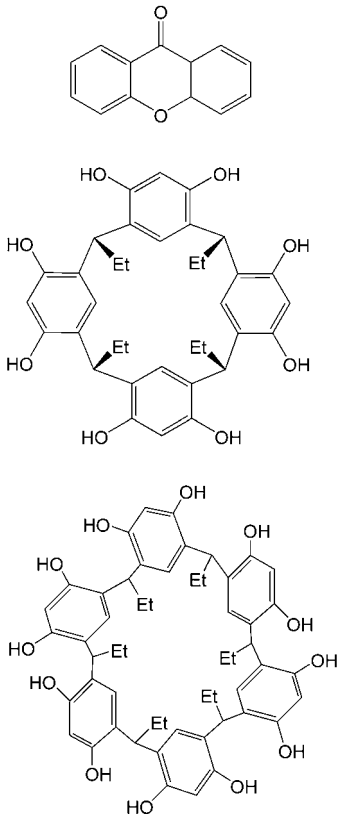

Scheme 1. The structures of xanthone (top), CECR (middle) and HECR (bottom).

Results and Discussion

Syntheses: CECR·xanthone·MeOH (**1**), and HECR·2 xanthone·6 MeOH (**2**) were prepared by hydrothermal synthesis, previously used successfully to prepare novel resorcinarene-based supramolecular frameworks incorporating aromatic ketones.[13,14,16] We did not succeed in preparing a CMCR·xanthone (CMCR = *C*-methylcalix[4]resorcinarene) phase, even though the composition of the corresponding reaction mixture was varied in a series of experiments. To allow comparison of the spectroscopic properties, the crystals of neat xanthone,[19] CECR, and HECR[20] were grown from open solutions, characterized by X-ray crystallography, and examined spectroscopically.

Crystal structures: The CECR molecules in **1** adopt the bowl-shaped (*r-cis-cis-cis*) conformation with four intramolecular hydrogen bonds along the upper rim (O···O = 2.682(2)–2.732(2) Å, Table S1 in the Supporting Information). Adjacent CECRs are connected by intermolecular hydrogen bonds (O···O = 2.688(2)–3.294(2) Å) to form layers parallel to the (100) plane with the deep bowl-shaped cavities, in which the CECRs are oriented in an up-and-down fashion (Figures 1 and S1 in the Supporting Information). Adjacent hydrogen-bonded layers are juxtaposed along the *a* axis such as to leave a void of 5.90 Å when the van der Waals radii of the atoms are taken into account (often referred to as the "effective separation"). The bowl-shaped cavities occupy 32.9 % of the crystal volume.[21] A fully ordered xanthone molecule is entrapped within each such cavity. No strong intermolecular interactions occur between xanthone and the host framework. One methanol molecule is included at the top of each cavity and is hydrogen-bonded to the hydroxyl oxygen atom (O–H···O = 2.678(2) Å) of an adjacent CECR.

As in HECR·12 DMSO, the HECR molecules in **2** adopt the *r-trans-cis-trans-cis-trans* conformation.[22] Adjacent HECR units are connected by intermolecular hydrogen bonds (O···O = 2.6925(9)–2.9011(9) Å), resulting in a one-dimensional wavy hydrogen-bonded chain parallel to the *b* axis (Figures 2 and S2 in the Supporting Information). These hydrogen-bonded chains are juxtaposed along the *a* axis with a 3.01 Å effective separation and along the *b* axis with a 4.91 Å effective separation. Channels along the *c* axis account for 39.6 % of the crystal volume. In each unit cell, two xanthone molecules are embedded in each channel as dimers, formed by π–π interactions between two aromatic rings with an interplanar distance of 3.41 Å. Six methanol molecules are clathrated in each channel to fill the gap left by the xanthone and are hydrogen-bonded to the hydroxyl oxygen atoms (O–H···O = 2.609(1)–2.969(1) Å) of the host network.

The most significant distinction between the two phases is that xanthone occurs as a monomer in **1**, whereas it is a dimer in **2**. The molecular dilution of xanthone is pronounced. Its concentration is 1.642 and 1.752 mol L^{-1} for **1** and **2**, respectively, compared with 7.106 mol L^{-1} in neat

© 2005 Wiley-VCH Verlag GmbH & Co. KGaA, Weinheim

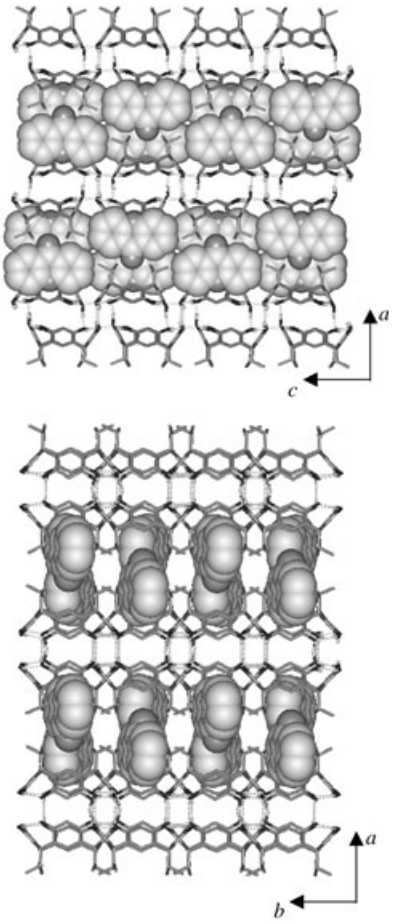

Figure 1. Three-dimensional supramolecular architecture of **1**, containing monomer xanthone viewed along the *b* axis (top), and viewed along the *c* axis (bottom). The methanol molecules are omitted for clarity.

xanthone crystals (Table 1).[19] Our calculations indicate that the xanthone dimer in the geometry found in crystals of **2** is less stable by 6.26 kcal mol^{-1} than two isolated monomers with the same geometry. On optimization, the interplanar distance increased by about 0.3 Å and a large lateral shift of about one ring occurred (Figure S3 in the Supporting Information), suggesting that such a dimer will not be found in solution. Nevertheless, it can be stabilized in the supramolecular environment as is evident from the crystal structure of **2**.

Table 1. Comparison of cavity size, concentration, and luminescence properties of xanthone in neat crystals and host–guest compounds.

	Volume per xanthone[a] [Å^3]	Concentration [mol L^{-1}, 90 K]	λ_{em} [nm, 17 K]	Lifetime [μs, 17 K]
neat xanthone	233.67	7.106	480	887
monomer in **1**	281.25	1.642	420	0.22
dimer in **2**	268.15	1.752	460	5.56

[a] Solvent molecules excluded in calculation of volume.

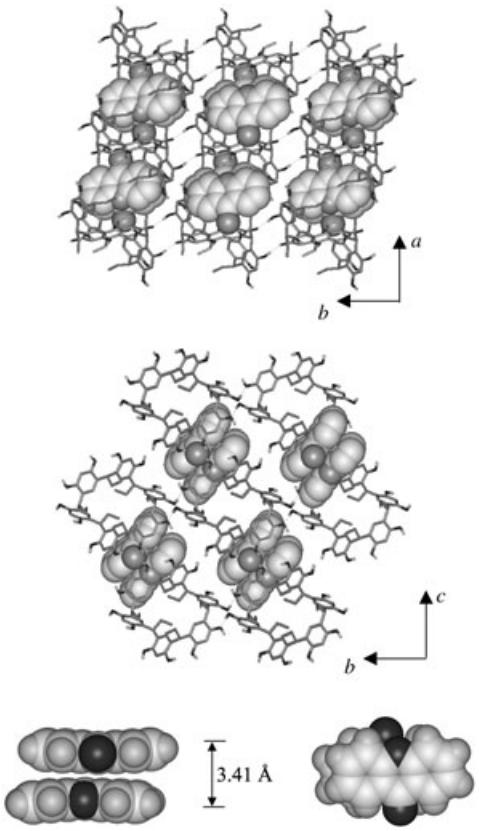

Figure 2. Three-dimensional supramolecular architecture of **2**, containing dimer xanthone viewed along the *c* axis (top), viewed along the *a* axis (middle), and side view (bottom left) and top view (bottom right) of the dimeric xanthone molecules connected by π–π interactions. The methanol molecules are omitted for clarity.

Whereas spectroscopic observations on solutions and computational results have been used extensively to obtain insight into the nature of excimers,[23–25] their dilute occurrence in supramolecular crystals opens the possibility of solid state studies of excimers, with spectroscopic and recently developed time-resolved diffraction methods.[26] The existence of a discrete monomer in **1** and discrete dimer of xanthone in **2** provide an opportunity to analyze the dependence of spectroscopic properties on molecular packing.

Spectroscopic properties

Absorption spectra: Similar to neat xanthone, the longest wavelength absorption bands of crystalline samples of both **1** and **2** occur at 335 nm (Figure 3). The longest wavelength absorption maxima in the UV-visible spectra may correspond to S_0–S_n transitions with $n>1$, as the S_0–S_1 transition may have a low oscillator strength.[23,27] Our TDDFT calculations (Table 2), indeed indicate that the lowest energy absorption maximum of **1** should be attributed to the S_0–S_2 transition (calcd wavelength 310.9 nm, oscillator strength 0.061), while the lowest energy absorption maxima of the dimer in **2** is assigned to the S_0–S_5 transition (calcd wavelength 310.5 nm, oscillator strength 0.094), as the transitions

 © 2005 Wiley-VCH Verlag GmbH & Co. KGaA, Weinheim

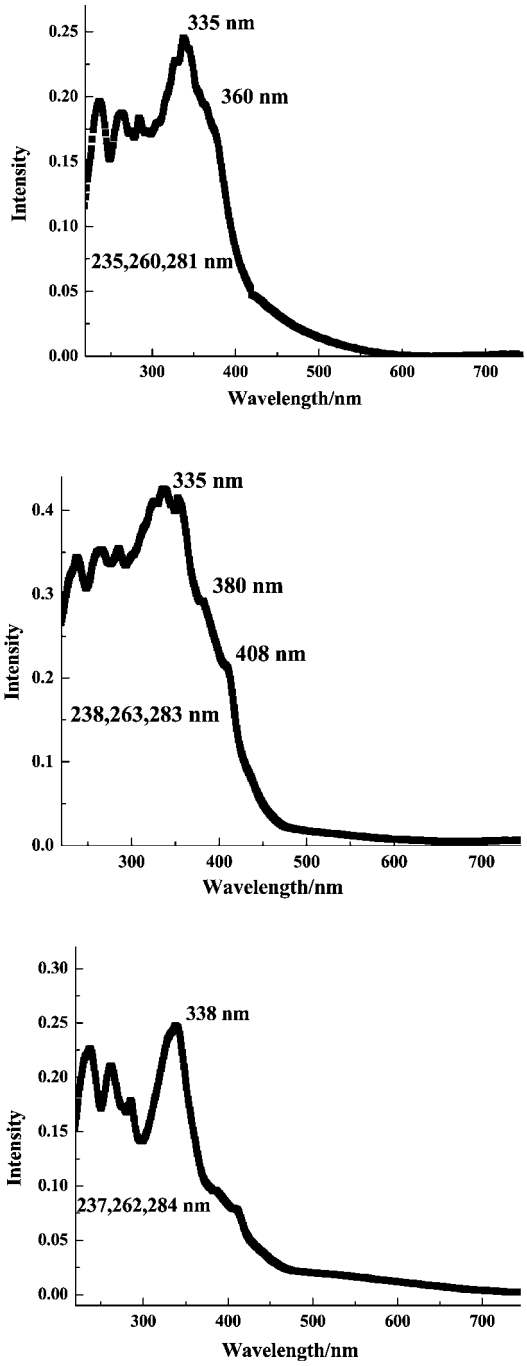

Figure 3. Solid-state UV-visible reflectance spectra of **1** (top), **2** (middle), and neat xanthone (bottom).

involving lower excited states have much lower oscillator strengths. The excited-state–ground-state (ES–GS) separations from the TDDFT calculations agree with the observed positions of the absorption bands.

Emission spectra: While the absorption spectra may vary little with degree of aggregation, as evident by comparison of the UV spectra of **1** and **2**, the emission spectra can be very sensitive.[28,29] Although the crystals of neat xanthone, which contain one-dimensional stacks with π–π interactions (Figure S4 in the Supporting Information),[19] emit at approximately 480 nm upon 366 nm excitation at 17 K, the luminescence maximum of monomer xanthone in **1** is found at about 420 nm, while the emission maximum of dimer xanthone in **2** occurs at 460 nm (Figure 4). This result is in agreement with the red-shifts commonly found in luminescence spectra of the excimer in solution,[23–25] and supported by our calculation of the energy-level spacings.

The emission spectrum of xanthone in hexane has been found to be strongly temperature dependent.[17] Only at very low temperature, below about 10 K, does emission from the $T_1(\pi,\pi^*)$ triplet state, which is close in energy to $T_2(n,\pi^*)$, become important. Based on TDDFT energy-level and molecular-orbital analyses, we similarly assign the triplet states of the monomer in **1** and the dimer in **2** to be of π,π^* nature for the T_1 state and of n,π^* nature for the T_2 state, as shown in Figure 5, the T_1–T_2 spacing being only 0.033 and 0.017 eV, respectively. Taking into account the temperature at which the current experiments were conducted (17 K) and the reported nonplanarity of the $T_1(\pi,\pi^*)$ state, which would be restrained in the crystal matrix, the luminescence in the supramolecular crystals is assigned to the $T_2(n,\pi^*)$ state.

Phosphorescence lifetimes: A major factor affecting solid-state photophysical behavior is energy transfer to the molecular environment, which shortens emission lifetimes or leads to full quenching of the emission through nonradiative decay of the excited species. Two mechanisms for energy transfer are distinguished.[30] The first, the Förster mechanism,[28,31] plays a major role in energy transfer in proteins and in solutions,[32] and is Coulombic in origin. It is the dominant factor in deactivation of excited singlet states at long distances (10 to 150 Å), and manifests itself in fluorescence quenching. For deactivation of triplet states Coulombic interactions that require triplet–triplet energy transitions (i.e., $^3D^* + {}^1A \rightarrow {}^1D + {}^3A^*$) on donor (D) and acceptor (A) are forbidden, and thus do not play a role. While short-range (< 10 Å) energy transfer is usually attributed to a Dexter exchange mechanism,[33] significant orbital-overlap-dependent exchange can also be mediated through charge-transfer (CT) configurations.[32,34] The exchange and CT couplings are short range as they depend on

Table 2. Calculated excited state energy separations and oscillator strengths of various linker molecules.

Energy separation	Monomer in **1** E [eV^{-1}] (f)	Dimer in **2** E [eV^{-1}] (f)	CECR E [eV^{-1}] (f)	HECR E [eV^{-1}] (f)
S_0–T_1	3.148 (0.000)	2.887 (0.000)	3.532 (0.000	3.575 (0.000)
S_0–S_1	3.710 (0.000)	3.622 (0.000)	4.083 (0.000)	4.262 (0.000)
S_0–S_2	3.988 (0.061)	3.623 (0.000)	4.254 (0.040)	4.270 (0.035)
S_0–S_3	4.730 (0.054)	3.900 (0.000)	4.297 (0.037)	4.397 (0.000)
S_0–S_4	5.059 (0.021)	3.948 (0.002)	4.429 (0.002)	4.399 (0.030)
S_0–S_5	5.249 (0.308)	3.993 (0.094)	4.620 (0.002)	4.582 (0.001)

© 2005 Wiley-VCH Verlag GmbH & Co. KGaA, Weinheim

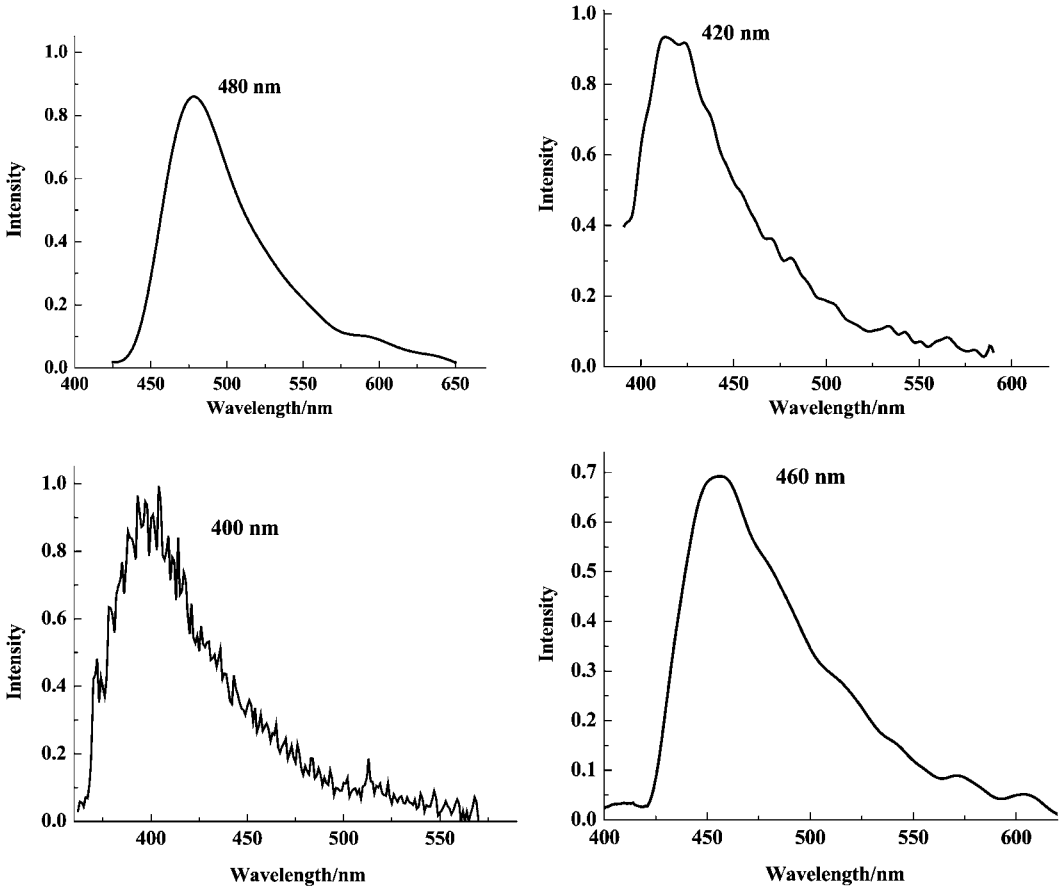

Figure 4. The emission spectra of xanthone in solid state at 17 K (top left), in hexane solution at room temperature (bottom left), in **1** (top right) and in **2** (bottom right) at 17 K.

overlap of donor and acceptor orbitals (in the supramolecular case the orbitals of the host molecules lining the guest cavity with the orbitals of the guest itself). Both the long- and short-range energy transfer depend on the energy-level spacings of the donor, which is deactivated, and the acceptor (Scheme 2).[23,30,32,35] The increased density of solids relative to solutions and the existence of well-defined host–guest geometries and interactions enhances the importance of the short-range mechanisms of luminescence quenching.

In a series of supramolecular solids based on resorcinarene and bipyridyl-type linker molecules, the intense phosphorescence of aromatic ketones was found to be completely[13,16] or very strongly quenched,[14] even at low temperature. Although we measured the lifetime of the neat xanthone crystal at 17 K as 887 μs, for **1** and **2** the corresponding numbers at the same temperature are only 0.22 and 5.56 μs, respectively, indicating that significant quenching occurs.

A necessary condition for energy transfer is matching of the spacings of the donor and acceptor energy levels affected by the transfer. While the absorption bands of powdered CECR or HECR crystals occur in the 210–400 nm region (Figure S4 in the Supporting Information), xanthone in its neat crystals emits at approximately 480 nm (Figure 4), suggesting that no significant overlap between the emission spectrum of guest and the absorption spectrum of host framework exists. However, the room temperature emission spectrum of xanthone dissolved in hexane is blue-shifted to approximately 400 nm (Figure 4). In addition, the longest wavelength absorption maxima in the UV spectra of CECR, and HECR correspond to S_0–S_n transitions with $n>1$, (Table 3) and are thus not characteristic for energy levels that can be involved in the short-range interactions. The TDDFT calculations on the isolated molecules indicate that the S_0–S_1 and S_0–T_1 separations of CECR or HECR are only slightly larger than those of the xanthone guest. When we take into account that the interactions in the solid state, such as hydrogen-bonding and π–π stacking, can further decrease the ES–GS separations of the host below the calculated values,[29] the energy gap of the host framework is likely to be similar to that of the xanthone guest, thus allowing significant energy transfer and corresponding quenching of the luminescence. As described above, for the dimer structure **2** the emission is significantly red-shifted and in agreement with calculated ES–GS separations. The observed reduction of luminescence quenching in **2** relative to **1** may thus be attributed to the reduced ES(triplet)–GS(singlet) energy gap of the xanthone donor, which becomes smaller than the corresponding gap of the host acceptor molecules.

 © 2005 Wiley-VCH Verlag GmbH & Co. KGaA, Weinheim

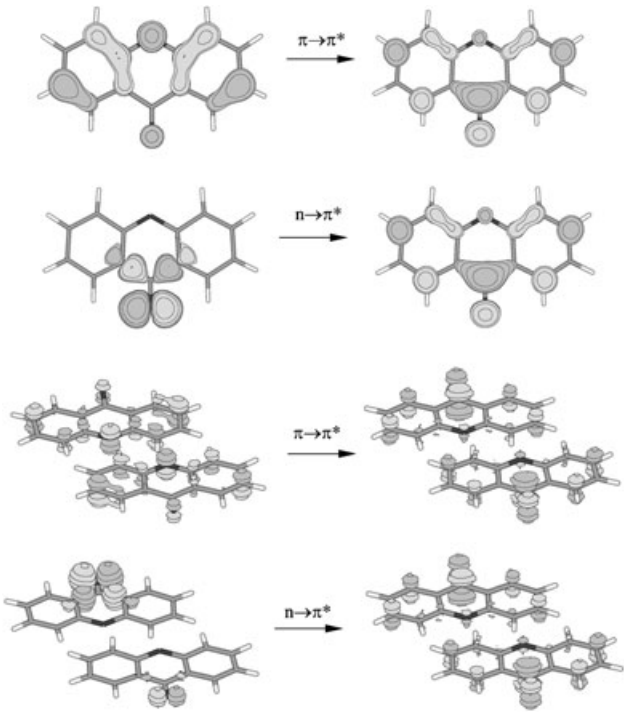

Figure 5. The contour plots of the relevant molecular orbitals of the monomer in **1** (top) and the dimer in **2** (bottom) in the $T_1(\pi,\pi^*)$ and $T_2(n,\pi^*)$ triplet state based on TDDFT energy level and molecular orbitals analyses. Isosurface drawn at 0.05 au.

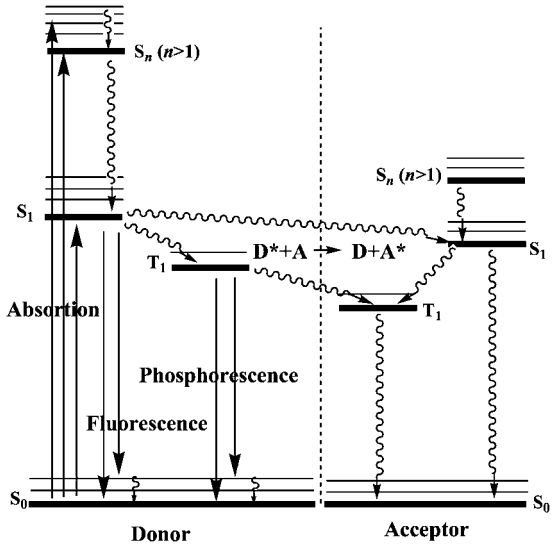

Scheme 2. Schematic of guest–host energy transfer mechanisms in crystalline supramolecular inclusion complexes. Straight arrows: radiative processes. Wavy arrows: nonradiative processes.

In a parallel study we have observed a similar increase in luminescence lifetime and an increased red-shift of the emission in a supramolecular solid containing a pyrene excimer.[36] On the other hand for excimers in solution, a decrease in the quantum yield of the luminescence is generally observed, resulting from an enhancement of self-quenching or concentration quenching when the concentration of a fluorescent species increases.[23] However, for excimers in the solid state, the lower ES–GS separation can suppress the competing energy transfer by increasing the difference in energy-level spacings between the guest and the host framework.

Table 3. Crystal data and structure refinement of **1** and **2**.

	1	**2**
formula	$C_{50}H_{52}O_{11}$	$C_{86}H_{100}O_{22}$
M_r	828.92	1485.66
crystal system	orthorhombic	triclinic
space group	*Pbcn* (No. 60)	$P\bar{1}$ (No. 2)
a [Å]	30.0636(14)	10.7903(5)
b [Å]	13.8059(7)	14.1835(7)
c [Å]	19.4867(9)	14.2469(7)
α [°]	90	117.322(1)
β [°]	90	90.147(1)
γ [°]	90	100.502(1)
V [Å^3]	8088.1(7)	1895.4(2)
Z	8	1
μ ($Mo_{K\alpha}$) [mm^{-1}]	0.095	0.093
reflns collected	118671	32294
independent reflns	9773	10483
R_{int}	0.0601	0.0208
data/parameters	9773/550	10483/688
goodness-of-fit on F^2	1.055	1.044
R_1 [$I>2\sigma(I)$]	0.0616	0.0378
wR_2 (all data)	0.1853	0.1119
$\Delta\rho_{max}/\Delta\rho_{min}$ [e Å^{-3}]	0.634/−0.576	0.505/−0.246

Concluding Remarks

Only few investigations of the electronic transitions involved in the photoluminescence and emission quenching in crystalline supramolecular systems have been carried out.[14] We find the intense phosphorescence of xanthone to be significantly quenched in the supramolecular solids examined, and the emission properies to be a function of the aggregation of the guest molecules. Examination of experimental host-absorption and guest-emission spectra and the TDDFT energy levels provides a basis for interpretation of the experimental results. The observed quenching contrasts with DCA·benzil (DCA = deoxycholic acid), in which the energy-level separation of the DCA host is significantly larger than that of the benzil guest molecules, and the phosphorescence lifetime of benzil at 17 K exceeds that of benzil in its neat crystal.[37]

Our results also confirm the crucial role of the energy-level separations in the energy transfer process. Energy-level separations can not be readily obtained from the absorption spectra, as the longest wavelength band observed often does not correspond to the S_0–S_1 transition, which may have low oscillator strength. With careful consideration of the factors involved, luminescent supramolecular systems can be designed by means of rational synthetic strategies.

© 2005 Wiley-VCH Verlag GmbH & Co. KGaA, Weinheim

Experimental Section

Synthesis of CECR·xanthone·MeOH (1): CECR (0.05 mmol, 30.0 mg), xanthone (0.05 mmol, 9.8 mg), and methanol:benzene (1:1, 4 mL) were sealed in a 6 mL Pyrex glass tube. The tube was allowed to stay at 120 °C for 30 h, followed by cooling to room temperature over 3 days. Yellow needle-shaped crystals appeared during the cooling period.

Synthesis of HECR·2 xanthone·6 MeOH (2): HECR (0.05 mmol, 45.0 mg), xanthone (0.10 mmol, 19.6 mg), and methanol:benzene (1:1, 4 mL) were sealed in a 6 mL Pyrex glass tube. The tube was allowed to stay at 120 °C for 30 h, followed by cooling to room temperature over 3 days. Yellow needle-shaped crystals appeared during the cooling period.

X-ray crystallography: Diffraction intensities for **1** and **2** were collected at 90 K on a Bruker Smart 1000 CCD area-detector diffractometer ($Mo_{K\alpha}$, $\lambda = 0.71073$ Å). The data were integrated, scaled, sorted, and averaged using the SMART software package.[38] The structures were solved with direct methods and refined with full-matrix least-squares methods by using the SHELXTL program package.[39] Anisotropic thermal parameters were applied to all non-hydrogen atoms. Hydrogen atoms were generated at idealized positions. Crystal data as well as details of data collection and refinement for the complexes are summarized in Table 3, while hydrogen bond parameters are listed in Table S1 in the Supporting Information. Drawings were produced with Weblab Viewer Pro. 4.0.[40]

CCDC-266789 and CCDC-266790 contain the supplementary crystallographic data for this paper. These data can be obtained free of charge from the Cambridge Crystallographic Data Center *via* http://www.ccdc.cam.ac.uk/data_request/cif.

Theoretical calculations: The binding energies of the dimer xanthone in **2** were performed at the BLYP level with a TZP basis set, by employing the ADF 2004 suite of programs.[41]

TDDFT calculations were performed at the B3LYP level with a 6–31G** basis set, by employing the Gaussian03 suite of programs.[42] Starting with the X-ray geometries, the structures were optimized by energy minimization. The contour plots of molecular orbitals were described with the Molden 3.9 graphic program.[43]

UV-visible reflectance and photoluminescence spectroscopy: UV-visible absorption experiments were performed on a Perkin–Elmer Lambda 35 UV-visible spectrometer equipped with an integrating sphere for diffuse reflectance spectroscopy. The spectra were collected in the 210–800 nm range at room temperature. Powdered crystals homogeneously diluted with a nonabsorbing matrix (MgO) and gently tapped into a sample holder were used as samples.

Photoluminescence measurements were carried out on a home-assembled emission detection system. Samples (several small single crystals) were mounted on a copper pin attached to a DISPLEX cryorefrigerator. A metallic vacuum chamber with quartz windows is attached to the cryostat, the chamber was evacuated to approximately 10^{-7} bar with a turbomolecular pump, which allows cooling down to about 17 K. The crystals were irradiated with 366 nm light from a pulsed N_2-dye laser. The emitted light was collected by an Oriel 77348 PMT device, positioned at 90° to the incident laser beam, and processed by a LeCroy Digital Oscilloscope with 1–4 GHz sampling rate.

Acknowledgements

We would like to thank Dr. Irina Novozhilova for help with the theoretical calculations, and Dr. Andrey Kovalesky for helpful comments. Support of this work by the Petroleum Research Fund of the American Chemical Society (PRF32638 AC3) and the National Science Foundation (CHE0236317) is gratefully acknowledged.

[1] "Fluorescence Studies of Supramolecular Host–Guest Inclusion Complexes": B. D. Wagner in *Handbook of Photochemistry and Photobiology* (Ed.: H. S. Nalwa) American Scientific, Stevenson Ranch, CA **2003**, pp. 1–57.

[2] F. Cramer, W. Saenger, H.-C. Spatz, *J. Am. Chem. Soc.* **1967**, *89*, 14–20.

[3] a) G. Patonay, A. Shapira, P. Diamond, I. M. Warner, *J. Phys. Chem.* **1986**, *90*, 1963–1966; b) J. B. Zung A. M. de la Peòa, T. T. Ndou, I. M. Warner, *J. Phys. Chem.* **1991**, *95*, 6701–6706; c) H. Yang, C. Bohne, *J. Phys. Chem.* **1996**, *100*, 14533–14539, and references therein.

[4] M. Barra, C. Bohne, J. C. Scaiano, *J. Am. Chem. Soc.* **1990**, *112*, 8075–8079.

[5] F. V. Bright, G. C. Catena, J. Huang, *J. Am. Chem. Soc.* **1990**, *112*, 1343–1346.

[6] S. K. Lower, M. A. El-Sayed, *Chem. Rev.* **1966**, *66*, 199–241.

[7] M. Sudhakar, P. I. Djurovich T. E. Hogen-Esch, M. E. Thompson, *J. Am. Chem. Soc.* **2003**, *125*, 7796–7797.

[8] I. Tanaka, Y. Tabata, S. Tokito, *Chem. Phys. Lett.* **2004**, *400*, 86–89.

[9] a) P. Coppens, *Chem. Commun.* **2003**, 1317–1320; b) L. X. Chen, G. B. Shaw, I. Novozhilova, T. Liu, G. Jennings, K. Attenkofer, G. J. Meyer, P. Coppens, *J. Am. Chem. Soc.* **2003**, *125*, 7022–7034; c) P. Coppens, I. I. Vorontsov, T. Graber, A. Y. Kovalevsky, Y. S. Chen, M. Gembicky, I. V. Novozhilova, *J. Am. Chem. Soc.* **2004**, *126*, 5980–5981; d) P. Coppens, O. Gerlits, I. I. Vorontsov, A. Yu. Kovalevsky, Y.-S. Chen, T. Graber and I. V. Novozhilova, *Chem. Commun.* **2004**, 2144–2145.

[10] P. Coppens, B.-Q. Ma, O. Gerlits, Y. Zhang, P. Kulshrestha, *CrystEngComm* **2002**, *4*, 302–309.

[11] a) J. W. Steed, J. L. Atwood, *Supramolecular Chemistry*, Wiley, Chichester, **2000**; b) G. R. Desiraju, *Crystal Design: Structure and Function*, Wiley, Chichester, **2003**; c) P. Erk, H. Hengelsberg, M. F. Haddow, R. van Gelder, *CrystEngComm* **2004**, *6*, 474–483.

[12] a) F. Wilkinson, P. A. Leicester, L. F. V. Ferreira, V. M. M. R. Freire, *Photochem. Photobiol.* **1991**, *54*, 599–608; b) L. F. Vieira Ferreira, I. Ferreira Machado, A. S. Oliveira, M. R. Vieira Ferreira, J. P. Da Silva, J. C. Moreira, *J. Phys. Chem. B.* **2002**, *106*, 12584–12593, and references therein.

[13] B.-Q. Ma, Y. Zhang, P. Coppens, *J. Org. Chem.* **2003**, *68*, 9467–9472.

[14] a) B.-Q. Ma, L. F. Vieira Ferreira, P. Coppens, *Org. Lett.* **2004**, *6*, 1087–1090; b) "The Emission Quenching of Benzil in Crystalline *C*-Methylcalix[4]Resorcinarene-Based Inclusion Complexes": S.-L. Zheng, P. Coppens, unpublished results.

[15] L. F. Vieira Ferreira, I. Ferreira Machado, J. P. Da Silva, A. S. Oliveira, *Photochem. Photobiol. Sci.* **2004**, *3*, 174–181, and references cited therein.

[16] B.-Q. Ma, P. Coppens, *Cryst. Growth Des.* **2004**, *4*, 1377–1385.

[17] a) M. Vala, J. Hurst, *Molecular physics* **1981**, *43*, 1219–1234; b) R. E. Connors, W. R. Christian, *J. Phys. Chem.* **1982**, *86*, 1524–1528.

[18] a) J. C. Scaiano, *J. Am. Chem. Soc.* **1980**, *102*, 7747–7753; b) M. Barra, C. Bohne, J. C. Scaiano, *J. Am. Chem. Soc.* **1990**, *112*, 8075–8079; c) M. Barra, C. Bohne, J. C. Scaiano, *Photochem. Photobiol.* **1991**, *54*, 1–5.

[19] Xanthone: $P2_12_12_1$, $a = 13.450$, $b = 14.060$, $c = 4.780$ Å, which is similar to that in S. C. Biswas, R. K. Sen, *Indian J. Pure Appl. Phys.* **1982**, *20*, 414–415.

[20] S.-L. Zheng, P. Coppens, unpublished results: CECR·CH_3CN·$4H_2O$: $P2/n$, $a = 13.7836$, $b = 7.7986$, $c = 18.2581$ Å, $\beta = 103.157°$; HECR-H_2O-MeOH: $R\bar{3}$, $a = 15.5571$, $b = 15.5571$, $c = 21.3445$ Å.

[21] A. L. Spek, PLATON, A Multipurpose Crystallographic Tool, Untrecht University, Utrecht (The Netherlands), **2003**.

[22] B. W. Purse, A. Shivanyuk, J. Rebek, Jr., *Chem. Commun.* **2002**, 2612–2613.

[23] J. M. Klessinger, J. Michl, *Excited States and Photochemistry of Organic Molecules*, VCH, New York, **1995**.

[24] E. C. Lim, *Acc. Chem. Res.* **1987**, *20*, 8–17.

 © 2005 Wiley-VCH Verlag GmbH & Co. KGaA, Weinheim

[25] "Structure Aspects of Exciplex Formation": F. Brouwer in *Conformational Analysis of Molecules in Excited States* (Ed.: J. Waluk), Wiley-VCH, Weinheim, **2000**, pp. 177–236, and references therein.
[26] "Photoinduced Formation of a Transient Intermolecular Cu–Cu Bond in a Substituted [{Cu-pyrazolate}$_3$] Crystal": P. Coppens, I. I. Vorontsov, A. Yu. Kovalevsky, Y.-S. Chen, T. Graber, I. V. Novozhilova, unpublished results.
[27] N. J. Turro, K.-C. Liu, M.-F. Show, P. Lee, *Photochem. Photobiol.* **1978**, *27*, 523–529.
[28] B. W. Meer, *Resonance Energy Transfer: Theory and Data*, VCH, New York, **1994**.
[29] a) P. Cassoux, *Science* **2001**, *291*, 263–264; b) S.-L. Zheng, J.-P. Zhang, W.-T. Wong, X.-M. Chen, *J. Am. Chem. Soc.* **2003**, *125*, 6882–6883; c) S.-L. Zheng, J.-P. Zhang, X.-M. Chen, Z.-L. Huang, Z.-Y. Lin, W.-T. Wong, *Chem. Eur. J.* **2003**, *9*, 3888–3896; d) S.-L. Zheng, X.-M. Chen, *Aust. J. Chem.* **2004**, *57*, 703–712.
[30] B. Valeur, *Molecular Fluorescence: Principles and Applications*, Wiley-VCH, Weinheim, **2002**.
[31] "Delocalized Excitation and Excitation Transfer": T. Förter, in *Modern Quantum Chemistry*, *Vol. 3* (Ed.: O. Sinanoglu) Academic Press, New York, **1965**, pp. 93–137.
[32] D. L. Andrews, A. A. Demidov, *Resonance Energy Transfer*, Wiley, Chichester, **1999**.
[33] D. L. Dexter, *J. Chem. Phys.* **1953**, *21*, 836–850.
[34] a) R. D. Harcourt, G. D. Scholes, S. Speiser, *J. Chem. Phys.* **1996**, *105*, 1897–1901; b) R. D. Harcourt, G. D. Scholes, K. P. Ghiggino, *J. Chem. Phys.* **1994**, *101*, 10521–10525.
[35] N. J. Turro, *Modern Molecular Photochemistry*; University Science Books, Sausalito, CA, **1991**.
[36] "Pyrene as a Guest in Supramolecular Solids": B.-Q. Ma, P. Coppens, unpublished results.
[37] "On the Design of Supramolecular Host/Guest Solids with Intense Guest Luminescence": S.-L. Zheng, P. Coppens, unpublished results.
[38] SMART and SAINTPLUS-Area Detector Control and Integration Software, Madison, WI, **2004**.
[39] G. M. Sheldrick, SHELXTL 6.10, Bruker Analytical Instrumentation, Madison, Wisconsin (USA), **2000**.
[40] Weblab Viewer Pro. 4.0, Molecular Simulations Inc., San Diego, CA, **1997**.
[41] G. te Velde, F. M. Bickelhaupt, S. J. A. Van Gisbergen, C. Fonseca Guerra, J. G. Baerends, T. J. Ziegler, *J. Comput. Chem.* **2001**, *22*, 931–967.
[42] M. J. Frisch, G. W. Trucks, H. B. Schlegel, G. E. Scuseria, M. A. Robb, J. R. Cheeseman, V. G. Zakrzewski, J. A. Jr., Montgomery, R. E. Stratmann, J. C. Burant, S. Dapprich, J. M. Millam, A. D. Daniels, K. N. Kudin, M. C. Strain, O. Farkas, J. Tomasi, V. Barone, M. Cossi, R. Cammi, B. Mennucci, C. Pomelli, C. Adamo, S. Clifford, J. Ochterski, G. A. Petersson, P. Y. Ayala, Q. Cui, K. Morokuma, D. K. Malick, A. D. Rabuck, K. Raghavachari, J. B. Foresman, J. Cioslowski, J. V. Ortiz, B. B. Stefanov, G. Liu, A. Liashenko, P. Piskorz, I. Komaromi, R. Gomperts, R. L. D. Martin, J. Fox, T. Keith, M. A. Al-Laham, C. Y. Peng, A. Nanayakkara, C. Gonzalez, M. Challacombe, P. M. W. Gill, B. Johnson, W. Chen, M. W. Wong, J. L. Andres, C. Gonzalez, M. Head-Gordon, E. S. Replogle, J. A. Pople, GAUSSIAN03, Revision C.02; Gaussian, Pittsburgh, PA, **2003**.
[43] G. Schaftenaar, Molden, Version 3.9, CAOS/CAMM Center Nijmegen, Toernooiveld, Nijmegen (Netherlands), **2003**.

Received: January 12, 2005
Published online: April 7, 2005

© 2005 Wiley-VCH Verlag GmbH & Co. KGaA, Weinheim